Environmental Processes (2019) 6:819–840
https://doi.org/10.1007/s40710-019-00401-x

ORIGINAL ARTICLE

# Removal of COD from Industrial Biodiesel Wastewater Using an Integrated Process: Electrochemical-Oxidation with $IrO_2$-$Ta_2O_5$/Ti Anodes and Chitosan Powder as an Adsorbent

D. P. Myburgh[1] · M. Aziz[1] · F. Roman[1] · J. Jardim[1] · S. Chakawa[1]

Received: 26 March 2019 / Accepted: 2 October 2019 / Published online: 9 November 2019


**Abstract**
The production of biodiesel is an energy and water-intensive process that produces wastewater with high concentrations of COD, BOD, and FOG. Conventional treatment processes are not capable of treating contaminants and pollutants in biodiesel wastewater to satisfactory concentrations, and hence, advanced treatment processes are necessary. Untreated discharge of biodiesel wastewater results in additional costs during the production of biodiesel when penalties and fines are applied. In this research, a lab-scale integrated treatment process was used to investigate the successful abatement of contaminants, COD, BOD and FOG, present in industrial biodiesel wastewater. The integrated treatment process consisted of three consecutive steps: acidification, electrochemical oxidation, and adsorption. Acidification as a pre-treatment occurred at a pH of 2. Electrochemical oxidation using $IrO_2$-$Ta_2O_5$/Ti anodes at a current density of 1 mA/cm$^2$ and NaCl concentration of 0.08 M was followed by three consecutive adsorption stages using Chitosan powder at a concentration of 4.5 g/L. The experimental results show that the integrated treatment process could reduce COD, BOD and FOG levels by 94%, 86% and 95%, respectively. The treated effluent complies with local industrial effluent discharge standards, which could be disposed of safely without further treatment.

**Keywords** Biodiesel wastewater · Electrochemical oxidation · Adsorption · Chitosan · MMO anode · COD removal

✉ M. Aziz
azizm@cput.ac.za

[1] Faculty of Engineering and the Built Environment, Department of Chemical Engineering, Cape Peninsula University of Technology, Bellville 7435 Cape Town, Republic of South Africa

## 1 Introduction

Threats to the environment in terms of oil pollution are related to industrial activities. These include extraction of fossil fuels, refinement thereof as well as the processing of foodstuffs, amongst others. Environmental problems are created worldwide when substances contaminated with oil are discharged into the environment (Ahmad et al. 2005; Sokker et al. 2011). Industrial oil wastewater (WW) such as biodiesel wastewater (BDWW) contains various contaminants as well as a characteristic emulsion consisting of oil and water. Alternative fuels, such as biodiesel, should serve as a link between sustainable development, the efficient conversion and use of energy and environmental preservation (Haseeb et al. 2011). Biodiesel is renewable, bio-degradable, non-toxic and possesses properties close to that of diesel fuel, and can be produced from vegetable oil as well as animal fats (Fazal et al. 2011).

Estimated global biodiesel production will increase from 30.1 million $m^3$ in 2015 to 41.1 million $m^3$ by the year 2025 (Foley et al. 2015), with current demands being met through the conventional alkali-catalyzed transesterification process (Jaruwat et al. 2010). The production of biodiesel is a process that consumes a lot of water and energy. This results in additional economic costs and puts a strain on the environment. When the wet washing process is used to remove excess contaminants, large amounts of highly polluted wastewater are created (Ngamlerdpokin et al. 2011). The wet washing process removes excess contaminants and impurities using water. This highly polluted effluent contains soap, catalyst, free glycerol, residual alcohol, water, biodiesel and free fatty acids (Daud et al. 2014). It is reported that for 1 L of biodiesel, 0.2-3 L wastewater is generated which is characterized by an alkaline pH, high concentrations of chemical oxygen demand (COD), biochemical oxygen demand (BOD) and fats, oils and greases (FOG) (Veljković et al. 2014). Together with low concentrations of nitrogen and phosphorus, this creates an unsuitable environment for microbial growth, and therefore, makes the wastewater difficult to degrade naturally. Wastewater containing water-oil emulsions may lead to difficulties during treatment stages and should be removed in order to prevent interfaces in water treatment units, avoid problems in biological treatment stages and comply with water discharge requirements (Sokker et al. 2011).

Veljković et al. (2014) list various processes that have been studied for the treatment of biodiesel wastewater, such as coagulation/flocculation (Daud et al. 2015), electroflotation (Mohtashami and Shangh 2019), dissolved air flotation (Rattanapan et al. 2011), electrocoagulation (Ngamlerdpokin et al. 2011; Chavalparit and Ongwandee 2009), biological treatment (Suehara et al. 2005; Siles et al. 2010), microbial fuel cell (Sukkasem et al. 2011) and integrated treatment processes (Costa et al. 2017). However, Dewil et al. (2017) classify physicochemical and biological treatment technologies as matured and therefore new technologies are needed to improve the treatment efficiency and abide by more stringent environmental regulations. Given that conventional treatment processes are less efficient, the scientific community set out in search of novel processes and operating conditions which could increase treatment efficiency of wastewater. Advanced Oxidation Processes (AOP) such as photocatalysis (Sharma and Philip 2016), Fenton processes (Xu et al. 2016), ozonation (Dewil et al. 2017), Anodic Oxidation (Moreira et al. 2017) and electrochemical oxidation are processes that rely on the production of reactive hydroxyl radicals. The Electrochemical Oxidation (EO) process is based on the in situ generations of the hydroxyl radical (•OH); the detailed electro-generation of •OH can be found in the work of Comninellis, (1994). After fluorine, the hydroxyl radical is the strongest oxidizing species with a high standard reduction potential. This allows it to non-selectively react with most organics which ultimately results in

their complete or partial mineralization to $CO_2$, water and inorganic ions (Comninellis 1994; Garcia-Segura and Brillas 2011).

The addition of chloride ions can increase the performance of organic removal through the interaction of active chlorine in the oxidation process. When chloride anion is oxidised on the anode surface, it releases chlorine. Electro generated chlorine diffuses away from the anode and is hydrolysed yielding HClO and $Cl^-$ through disproportionation, with hypochlorous acid in acid-base equilibrium with hypochlorite anion species (Garcia-Segura et al. 2018; Rajkumar et al. 2005; Rajkumar and Palanivelu 2004). Mixed Metal Oxide (MMO) anodes have been studied for applications related to semiconductors, sensors, photoconductive thin films and especially electrode materials. The application of MMOs as the anode for the removal of persistent organic pollutants; present in water; has made notable progress in research (Wu et al. 2014). The mixed oxides of $IrO_2$-$Ta_2O_5$ on a Ti substrate, or $IrO_2$-$Ta_2O_5$/Ti, show high electrical conductivity, are electrochemically active and are known for their long service life, therefore, they have been used for various applications including wastewater treatment and electroplating. $IrO_2$-$Ta_2O_5$/Ti anodes are classified as dimensionally stable anodes (DSA) and are an effective electron sink when used during anodic reactions; these anodes show very little or no loss in dimensions (Huang et al. 2017). Furthermore, the use of Ti-based $IrO_2$–$Ta_2O_5$ coated anodes grew substantially in the past given their stability and durability under extreme operating conditions. $IrO_2$–$Ta_2O_5$ coatings are usually prepared by thermal decomposition since it is low in cost and fairly uncomplicated (Yan et al. 2015).

This work focuses on the improvement of electrochemical oxidation and adsorption processes for cleaning biodiesel wastewater before discharging it to the receiving environment. The studies have been done at laboratory scale at ambient temperatures by an integrated treatment process consisting of three consecutive treatment steps: (1) acidification; (2) electrochemical oxidation using $IrO_2$–$Ta_2O_5$ anodes and (3) adsorption using chitosan as an adsorbent. The electrochemical oxidation of biodiesel wastewater was investigated at the start in order to determine the operating conditions that would result in the maximum COD removal. The same methodology was applied to the adsorption process. After the operating parameters of these two individual processes were established and pollutant removal was confirmed, they were combined as consecutive steps in order to remove % of COD, FOG and BOD from industrial biodiesel wastewater.

## 2 Materials and Methods

Crude industrial biodiesel wastewater was collected from a commercial biodiesel producer operating in Cape Town, South Africa. The wastewater was collected when available, and therefore, varied slightly in composition. The collected wastewater was labelled and stored in 5 L amber flasks in the fridge. The discharge of industrial biodiesel wastewater in the City of Cape Town (CCT) is regulated by the "City of Cape Town: Wastewater and Industrial Effluent By-law, 2013". Pollutant concentrations required by the CCT, compared to those present in industrial biodiesel wastewater in this research is shown in Table 1.

### 2.1 Water Chemistry Analysis

The COD concentration was determined by Chromosulfuric acid oxidation method using Merck reagents. The TR 420 Thermo-reactor was used for digestion. The NOVA 60

**Table 1** Pollutant concentrations in biodiesel wastewater

| Parameter | Unit | Tested Research Value | CCT: Requirements |
|---|---|---|---|
| COD | mg/L | 55,000–65,000 | 5000 |
| FOG | mg/L | 500–550 | 4000 |
| BOD | mg/L | 38,000–40,000 | – |
| Salinity | g/L | 2.03 | – |
| EC | mS/cm | 3.5 | 500 |
| TDS | g/L | 2.3 | 4 |
| pH | – | 9.8 | 5.5–12 |
| Turbidity | NTU | 380 | – |

photometer was used to determine the COD concentration photometrically. The Crison CM 35+ was used to measure the EC, TDS and Salinity. The pH measured with HI8424 Portable pH/mV Meter, and an HF Scientific MicroTPI Infrared Turbidity Meter was used to measure the turbidity.

## 2.2 Acidification

As a pre-treatment, all wastewater collected for experimental use was acidified using $H_2SO_4$ at a final pH ranging between 1 and 6. Acidification occurred in a 6 L round bottom flask which was magnetically stirred at ambient conditions. The acidified wastewater was mixed for 2 h and allowed to stand for 12 h to ensure complete phase separation. The oil-rich top phase was removed from the remaining aqueous phase through slow decantation and was analyzed to quantify pollutant removal. All acidification experiments were duplicated.

## 2.3 Electrochemical Oxidation

The pre-treated biodiesel wastewater was subjected to electrochemical oxidation occurring in a 1 L glass reactor. Two commercial $IrO_2$–$Ta_2O_5$ anodes were used with a total surface area of 400 $cm^2$. The distances between the anodes were kept at 0.02 m. To ensure good mass transfer and a constant temperature of 60 °C, a magnetic heater/stirrer was used. Experiments were conducted and particles were generated galvanostatically by applying a constant current using a power supply (Manson SPS9400 Switching mode DC regulated power supply). During the treatment, process samples were taken in 2-h intervals and analyzed for water quality parameters including COD, EC, and pH following standard methods. The total reaction time for the electrochemical oxidation reaction was 100 h.

## 2.4 Adsorption

During the adsorption of organic compounds from biodiesel onto chitosan, the concentration of chitosan, initial pH and adsorption time were investigated. For the adsorption stage, the pH of the aqueous phase was adjusted to be within the preferred range of 2–6 by the addition of NaOH (Merck 106,498). Approximately 200 mL of BDWW was treated by the addition of chitosan powder at concentrations between 2.5, 3.5 and 4.5 g/L as the adsorbent in a glass beaker with a constant stirring rate of 350 rpm, for a selected adsorption time of 3 h.

The concentration of COD in the wastewater was measured every hour by taking a sample and filtering it with a 0.45 μm syringe filter and standard analyzing methodology was followed

thereafter. The treated wastewater was separated from the adsorbent by vacuum filtration through filter paper (No.1 Whatman WHA1001070). Fresh chitosan was used to repeat the adsorption stages. This was done three times. The experiments were duplicated to statistically validate the results.

### 2.5 Calculation of Instantaneous Current Efficiency (%ICE)

The Instantaneous Current Efficiency (ICE) was calculated to quantify the effect that current density and NaCl concentration has on the electrochemical oxidation process, according to Eq. (1):

$$\mathrm{ICE}(\%) = \frac{[\mathrm{COD}]_t - [\mathrm{COD}]_{t+\Delta t}}{8\,I\,\Delta\,t} F\,L \times 100 \quad (1)$$

where: t represents the electrolysis time; [COD]t represents the COD concentration at time t; [COD] t + Δt represents the COD concentration at t + Δt; I is the current density; F is the Faraday constant (96,485 C/mol), and L is the volume of wastewater in the electrochemical reactor L.

## 3 Results and Discussion

### 3.1 Acidification of Biodiesel Wastewater

Acidification of BDWW was carried out using $H_2SO_4$ at various pH values as indicated in Fig. 1. The addition of acid as a proton donor destabilizes the emulsion through the lessening of electrostatic forces which enables the coalescence of fine oil droplets into larger droplets (Veljković et al. 2014), resulting in phase separation. The water separated into 2 phases, an oil-rich layer at the top, and an aqueous phase at the bottom.

The oil-rich top layer had a similar colour to that of oil/biodiesel, whereas the residual aqueous phase has lower turbidity and reduced pollutant concentrations. 1.65–2.2% volume per volume (*v*/v) vegetable oil was removed in the pH range 1–3, however, insufficient amounts of oil 0.2–0.15% (v/v) was removed in the pH range 4–5, whereas no oil was

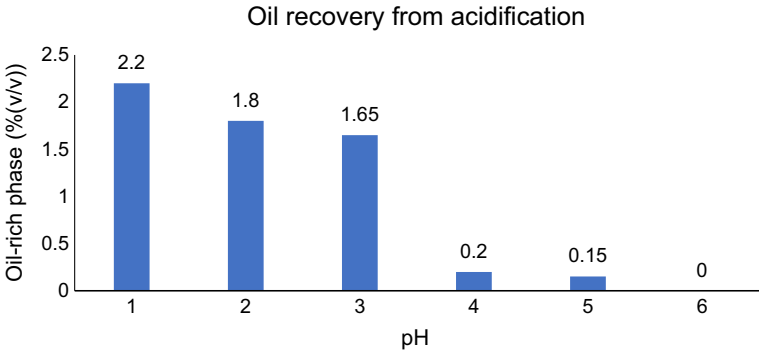


**Fig. 1** Oil removed through acidification

recovered under pH conditions ranging from 6 to 9. Therefore, acidic conditions are favourable for oil removal. Furthermore, acidification at a pH value of 2 was able to remove 11% of COD, 10% of BOD, 80% FOG and 70% turbidity as shown in Table 2. Other parameters such as TDS, EC and salinity showed a slight decrease.

Rattanapan et al., (2011) adjusted the pH of biodiesel wastewater to a value of 3 and found that it was sufficient for the removal of FOG and COD, reporting removal efficiencies of 80% and 45% respectively. Similarly, Ngamlerdpokin et al., (2011) report that higher levels of oil removal were achieved with a pH value ranging between 1 and 2.5. It is therefore clear that acidification plays a significant role as a pre-treatment step. Based on the result obtained, a wastewater pH of 2 was selected for subsequent experiments.

### 3.1.1 Effect of Current Density

The calculated ICE % values for experimental conditions with current densities 1, 2 and 4 mA/cm$^2$, respectively, are shown in Fig. 2. A current density of 1 mA/cm$^2$ achieved the highest ICE value of 3.3% at 2 h, after which it gradually decreased to 1.1% at 24 h. Current densities 2 and 4 mA/cm$^2$ achieved significantly lower ICE values of 1.7% and 0.3% respectively. It decreased to values lower than 0.2% during the 24-h period. Normally, the ICE (%) decreased with an increase in current density. Almomani and Baranova (2012) and Coledam et al. (2014) found that an increase in current density resulted in a decrease of ICE due to the side reaction of oxygen evolution and/or mass transport limitations. According to Wu et al. (2014) the oxygen evolution reaction is not favoured at lower current densities, which explains why higher ICE values were obtained at the lower current densities.

Based on the initial experimental runs, a current density of 1 mA/cm$^2$ showed favourable results and was chosen for subsequent experimental runs to determine the effect of NaCl as a supporting electrolyte.

### 3.1.2 Effect of NaCl Concentration

The effect of NaCl concentration (M) on the electrochemical oxidation at 1 mA/cm$^2$ was investigated by varying the NaCl concentration between 0 and 0.1 M. The calculated ICE % values for experimental runs DG are shown in Fig. 3.

The %ICE increased with an increase in NaCl concentration, thus, confirming the positive effect that NaCl has on the electrochemical oxidation of BDWW. A maximum of 28.5% and 26% efficiency was observed at 0.08 M NaCl and 0.1 M NaCl, respectively. An efficiency of 3.3% was observed when no NaCl was added. Coledam et al. (2014) reported that higher ICE

**Table 2** Characteristics of biodiesel wastewater after acidification at a pH value of 2

| Parameter | Unit | Initial Value | Acidified |
|---|---|---|---|
| COD | mg/L | 55,000–60,000 | 53,250 |
| FOG | mg/L | 500–550 | 106 |
| BOD | mg/L | 38,000–40,000 | 36,225 |
| Salinity | g/L | 2.03 | 1.5 |
| EC | mS/cm | 3.5 | 2.6 |
| TDS | g/L | 2.3 | 1.7 |
| pH | – | 9.8 | 2 |
| Turbidity | NTU | 380 | 100 |

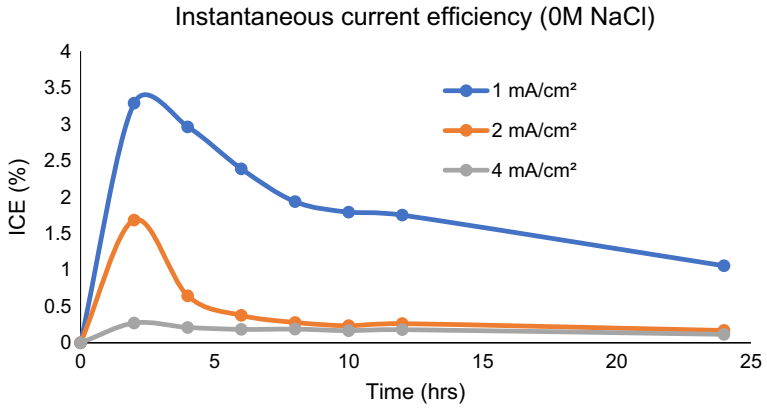


**Fig. 2** Instantaneous current efficiency - Effect of current density

values are observed in the presence of NaCl compared to that without. Based on the results obtained, a NaCl concentration of 0.08 M was chosen for all subsequent experimental runs.

## 3.2 Electrochemical Oxidation

### 3.2.1 The Effect of Current Density

The effect of current density on the electrochemical oxidation of BDWW using $IrO_2 - Ta_2O_5$ anodes was investigated over a range of 0.5–4 mA/cm$^2$ at an initial pH of 2 as shown in Fig. 4. Lower current densities in the range of 1–1.25 mA/cm$^2$ performed better than higher current densities of 2–4 mA/cm$^2$.

Figure 4, presents the COD results of experimental runs 1 (0.5 mA/cm$^2$), 2 (0.75 mA/cm$^2$), 3 (1.0 mA/cm$^2$), 4 (1.25 mA/cm$^2$), 5 (1.75 mA/cm$^2$) 6 (2.0 mA/cm$^2$) and 7 (4.0 mA/cm$^2$). It can be observed that for the first 40 h, the COD removal rate is almost similar for all experimental runs. After the 50-h mark, experimental run 3 (1.0 mA/cm$^2$) removal rate

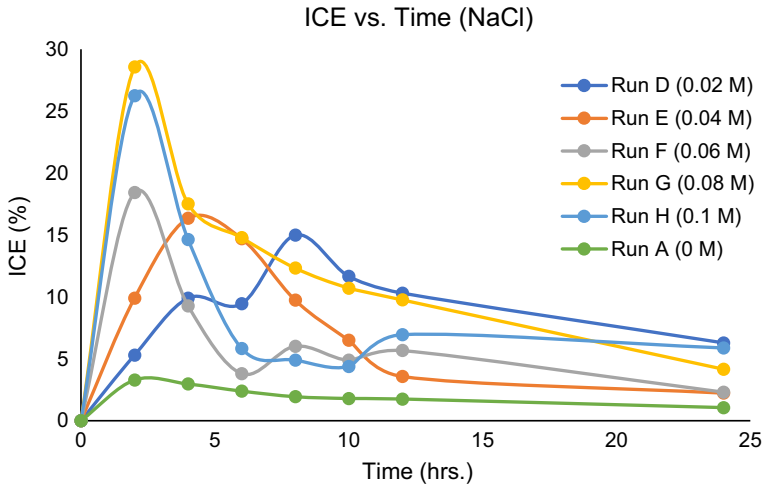


**Fig. 3** Instantaneous current efficiency - Effect of NaCl concentration

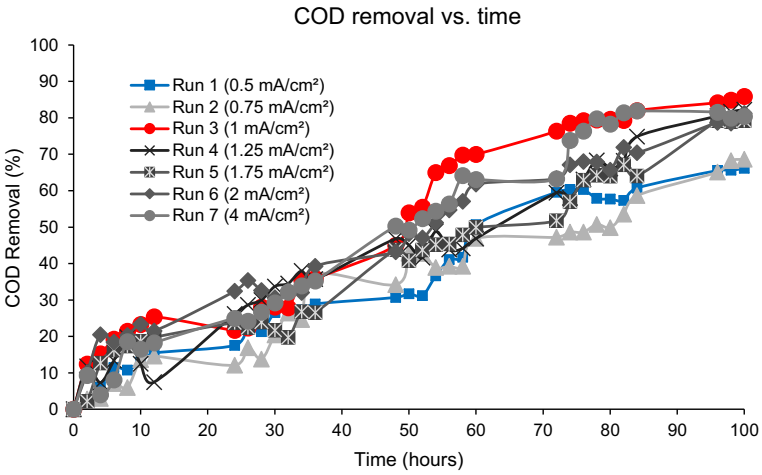


**Fig. 4** Effect of current density on COD removal

increases by almost 20% and removes more than 85% at the 100-h mark. Experimental runs 4 (1.25 mA/cm$^2$) and 5 (1.75 mA/cm$^2$) follow a similar trend, but at a lower rate. For experimental runs 2 (0.75 mA/cm$^2$), the % COD removal is the slowest.

Figure 5, presents the COD, BOD and FOG results of experimental runs 1 (0.5 mA/cm$^2$), 2 (0.75 mA/cm$^2$), 3 (1.0 mA/cm$^2$), 4 (1.25 mA/cm$^2$), 5 (1.75 mA/cm$^2$) 6 (2.0 mA/cm$^2$) and 7 (4.0 mA/cm$^2$). It can be observed that the experimental run 3 with a current density of 1.0 mA/cm$^2$ shows the highest removal of COD (85%), BOD (88%) and FOG (85%), whereas experimental run 1 with a current density of 0.5 mA/cm$^2$ shows the least removal. It can also be observed that removal efficiency for current density 2.0 and 4.0 mA/cm$^2$ is also quite significant. Wu et al. (2014) state that when high removal efficiencies have been reached, as shown in experimental run 3, the increase of current density thereafter will not have a significant effect as observed with experimental runs 6 and 7.

When comparing the smaller current density increments, the removal efficiencies at these conditions seems the same. However, it should be noted that the energy consumption at a current density of 1 mA/cm$^2$ is much lower and achieved the highest removal of COD, BOD and FOG. At the same operating conditions, as shown in Table 3, experimental run 4 with a

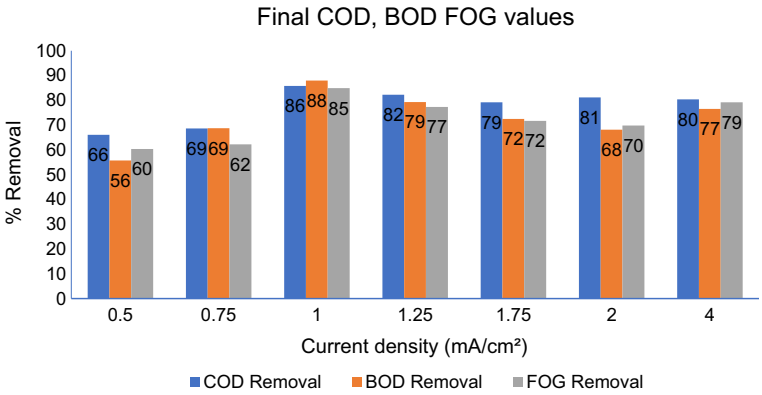


**Fig. 5** Final values for COD removal – Current density

current density of 1.25 mA/cm$^2$ achieved a COD removal efficiency of 82% with a final COD removal concentration of 9903 mg/L and similarly, experimental run 3 with a current density of 1.0 mA/cm$^2$ achieved a COD removal efficiency of 86% with a final COD removal concentration of 7086 mg/L, respectively. Therefore, increasing the current density, at small increments below or above 1 mA/cm$^2$ resulted in lower pollutant removal efficiencies.

The observed COD removal was due to the oxidation of organic pollutants to intermediate species and possible complete mineralization in the wastewater. Electro-oxidation of organic contaminants using $IrO_2 – Ta_2O_5$ active anodes (M) occurs through mediated oxidation in the bulk solution (Garcia-Segura et al. 2018). Comninellis et al., (2008) and Martínez-Huitle and Andrade, (2011) explain these trends by stating that that $IrO_2 – Ta_2O_5$ anodes are a good catalyst for the oxygen evolution side reaction and therefore only permit for the partial oxidation of organics since these anodes are classified as active anodes. However, the effective oxidation of pollutants is possible at lower current densities and longer electrolysis time, as shown with these results. Santos et al., (2006) studied the electrochemical oxidation of oily wastewater using a $Ru_{0.34}Ti_{0.66}O_2$ anode which falls into the same family as $IrO_2 – Ta_2O_5$ anodes, namely dimensionally stable anodes (DSA).

The operating temperature of 50 °C was similar to the temperature used in this research although higher current densities were applied. At a current density of 100 mA/cm$^2$ and 70 h of electrolysis, the system achieved 57% COD removal. The results obtained by Santos et al. (2006) were not significant in terms of COD removal. However, their results strengthen the notion that lower current densities are more favourable for COD removal when using this type of anodes.

### 3.2.2 The Effect of NaCl Concentration

NaCl was added at various concentrations between 0 and 0.1 M into the bulk of the electrochemical cell, as a supporting electrolyte. The aim of adding NaCl was to increase the removal of pollutants.

The influence of NaCl was investigated without any electrolyte added, and thereafter, by changing the NaCl concentration by increasing it by 0.02 M until a final experimental run of 0.1 M. Samples were taken every two hours to quantify COD, EC, TDS, Salinity, Turbidity, and pH. Fig. 6 shows the % COD removal over a 100-h time. Throughout this period, the influence that NaCl has on the removal rate of pollutants can be observed and more specifically, on COD removal. As the NaCl concentration increases, so does the % COD removal.

At a NaCl concentration of 0 M, a COD removal of 48.7% was achieved after 100 h. However, the addition of NaCl at a concentration of 0.06 M and 0.08 M yielded 78.5% and 86% COD removal, respectively. When the NaCl concentration further increased to 0.1 M similar yet slightly lower COD removal efficiency of 84% was observed, indicating that a NaCl concentration of 0.08 M is resulting in a maximum COD removal of 86%.

**Table 3** Final concentrations for COD, BOD and FOG - Additional experiments

| Current Density (mA/cm$^2$) | Final COD (mg/L) | Final BOD (mg/L) | Final FOG (mg/L) |
|---|---|---|---|
| Experimental run 2 (0.75) | 14,856 | 11,327 | 40 |
| Experimental run 3 (1) | 7086 | 4354 | 16 |
| Experimental run 4 (1.25) | 9903 | 7483 | 24 |
| Experimental run 5 (1.75) | 11,904 | 9966 | 30 |

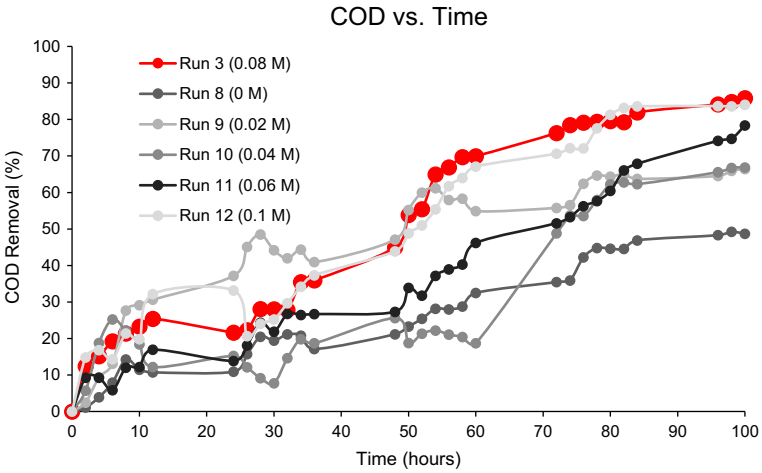


**Fig. 6** Effect of NaCl concentration on COD removal

Ltaïef et al., (2017) noted that the indirect oxidation of pollutants in wastewater is widely applied. This is due to active-chorine species, such as hypochlorous acid and hypochlorite that are generated by the anodic oxidation of chlorides. However, the addition of NaCl resulted in a decrease of total organic carbon, compared to when an inert supporting electrolyte ($Na_2SO_4$) was used. This could be attributed to the possible formation of oxidation-resistant chlorinated intermediates. Fajardo et al. (2017) found that the degradation rate of pollutants depends on the supporting electrolyte used. Similarly to the results obtained during this study, these authors (Ltaïef et al. 2017; Fajardo et al. 2017) also found that the addition of NaCl resulted in better degradation values. This behaviour was ascribed to the generation of diverse oxidizing species which were able to react directly or indirectly with the organic compounds.

The final % COD, BOD and FOG removal efficiencies are compared at various NaCl concentrations in Fig. 7. When NaCl concentration was at 0 M, final COD, BOD and FOG removals of 49%, 55% and 79%, were achieved, respectively. As the NaCl concentration increased to 0.08 M, the % COD, BOD and FOG removal reached a maxim of 86%, 88% and 85%, but at NaCl concentration of 0.1 M, the respective removals were 84%, 83% and 83%. These results reiterate that a NaCl concentration of 0.08 M is appropriate for maximum pollutant removal as stated above.

According to Rajkumar et al., (2005), Zhang et al., (2006) and Jaruwat et al., (2010), the NaCl as a supporting electrolyte can enhance pollutant removal by oxidizing organic compounds. This happens through the production of active chloro- species ($CL_2$/OCL) that are electrochemically generated by the oxidation of chloride ions to chlorine. For complete mineralization to occur, the reaction with water, need to produce hypochlorous acid that reacts and oxidizes pollutants to intermediate species or $CO_2$ and $H_2O$.

The final COD, BOD, and FOG concentration values for each experimental run are shown in Table 4. Experimental run 3 with a current density of 1 mA/cm$^2$ and NaCl concentration of 0.08 M achieved a final COD concentration of 7086 mg/L, which is better than what was achieved with a NaCl concentration of 0.1 M and final COD concentration of 8805 mg/L.

Figure 8 shows the mean energy usage at different current densities and are compared to the corresponding % COD removal. It was observed that the lowest mean energy consumption of 6.8 kWh/kg COD removed, occurred at a current density of 0.5 mA/cm$^2$, which corresponds to

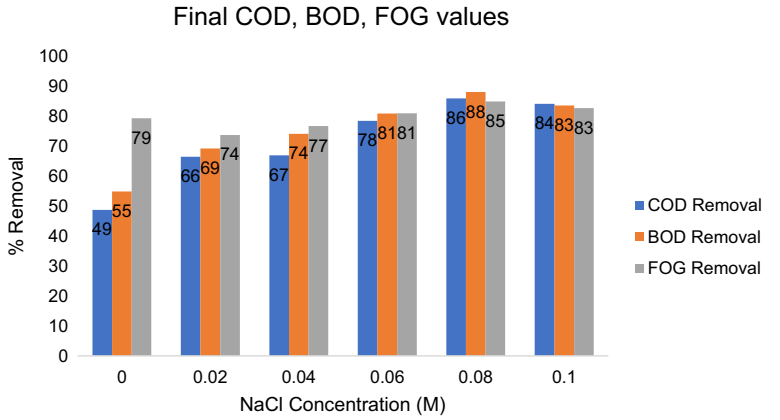


**Fig. 7** Effect of NaCl concentration of pollutant removal efficiencies

with a % COD removal of 66%. The current density of 1 mA/cm$^2$, which used double the energy of 13.5 kWh/kg COD removed, resulted in the highest COD removal of 86%.

Further increases in current density only amounted to more energy consumed with lower COD removal efficiencies.

## 3.3 Adsorption – Chitosan Powder

### 3.3.1 The Effect of pH

The effect of initial wastewater pH on the pollutant removal was investigated over a pH range 2, 4 and 6. The adsorbent, chitosan powder, was used at the following concentrations: 2.5, 3.5 and 4.5 g/L, respectively. A constant mixing rate of 350 rpm and adsorption time of 3 h per adsorption stage at ambient conditions were witnessed. The initial pH of the wastewater affects the surface chemistry of the adsorbent as well as the chemistry of the pollutants in the BDWW (Pitakpoolsil and Hunsom 2013).

Figure 9 shows adsorption capacities over the 3 pH ranges at a constant chitosan concentration of 3.5 g. It can be observed that the adsorption capacity of COD is at its highest of 147 mg/g at a pH of 2 and decreases as the pH increases, indicating that pollutants were better removed in more acidic conditions.

This can be explained by the hydrogen atom ($H^+$) in the solution, protonating the amine groups (-$NH^2$) in chitosan, resulting in interaction with anionic molecules. Sokker et al. (2011)

**Table 4** Final concentrations for COD, BOD & FOG – Electrochemical oxidation

| NaCl concentration (M) | Final COD (mg/L) (% Removal) | Final BOD (mg/L) (% Removal) | Final FOG (mg/L) (% Removal) |
|---|---|---|---|
| 0 | 25,184 (49) | 16,361 (55) | 22 (79) |
| 0.02 | 16,445 (66) | 11,188 (69) | 28 (74) |
| 0.04 | 13,832 (67) | 9410 (74) | 25 (77) |
| 0.06 | 10,230 (78) | 6959 (81) | 20 (81) |
| 0.08 | 7086 (86) | 4354 (88) | 16 (85) |
| 0.1 | 8805 (84) | 5990 (83) | 18 (83) |

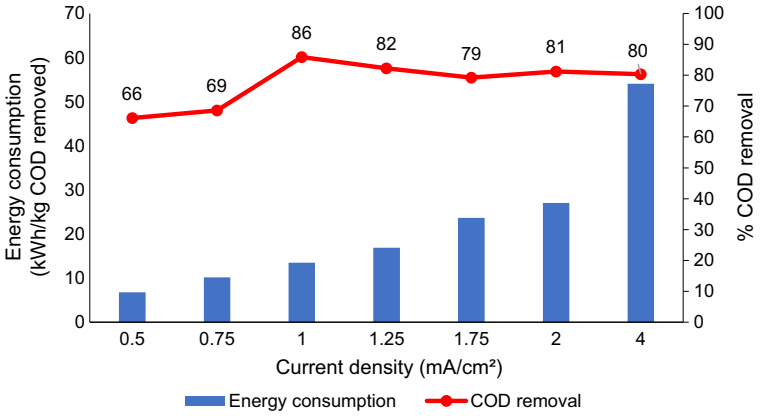


**Fig. 8** Mean energy consumption

reported that strong acidic conditions destabilize the oil molecules. Chitosan stimulates a physicochemical effect to demulsify and increase the droplet size that improves the adsorption of oil. Sakkayawong et al. (2005) and Ruhsing Pan et al. (1999) attribute the increase in chitosan adsorption capacity under acidic conditions to an increase in the number of protonated amine groups in the chitosan polymer. The Point of Zero Charge of Chitosan is at pH 6.3, and 99% of total amino groups are protonated at pH 4.3 (De Marques Neto et al. 2013). Therefore, the pH of 2 was identified for further experimental runs.

### 3.3.2 The Effect of Chitosan Concentration

The effect of the chitosan powder concentration on the adsorption capacity of COD was evaluated over a concentration range of 2.5, 3.5 and 4.5 g/L at a pH of 2. The adsorption capacity of COD increased significantly with corresponding adsorbent dosages (Fig. 10).

Figure 10 shows the results of adsorption capacity over adsorbent dosages. These experimental runs were over a 9-h period. Fresh chitosan powder was added after every 3 h at same dosage concentration as mentioned before. Figure 11 shows that equilibrium was reached after 3 h, indicating that the adsorbent reached its saturation point. Based on this observation, fresh Chitosan was added every 3 h. According to Pitakpoolsil and Hunsom (2013), the addition of fresh chitosan concentration assist in the increase of adsorption capacity at constant

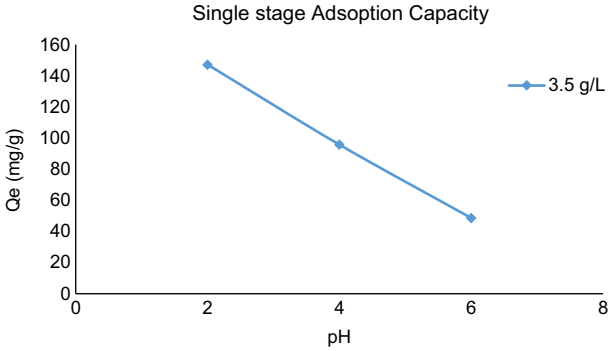


**Fig. 9** Effect of pH on single-stage adsorption capacity

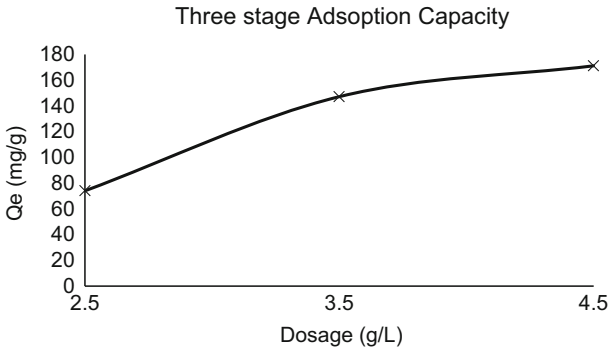


**Fig. 10** Multi-stage adsorption capacity

concentrations; however, the adsorption capacity of the chitosan decreases with each additional stage since the process becomes inefficient in the presence of low concentrations of pollutants. The maximum adsorption capacity of 171 mg/g was observed at a dosage of 4,5 g/L after three consecutive adsorption stages using fresh chitosan. Lower adsorption capacities of 137 mg/g and 71 mg/g were obtained at chitosan dosages of 3.5 g/L and 2.5 g/L, respectively.

Figure 11 presents % COD removal for the three dosage concentration stages for a 9-h period. At a dosage concentration of 4.5 g after 9 h, a maximum % COD removal of 55% was achieved. At lower dosages of 3.5 g and 2.5 g, lower % COD removal efficiencies of 40% and 35% were achieved, respectively. Thus, an increase in concentration dosage enhanced the adsorption capacity. Ahmad et al. (2005) found that an increase in chitosan dosage leads to an increase in oil removal; however, this is only true at low dosages since chitosan possesses a high charge density, and therefore, only low amounts are needed. Similarly, Thirugnanasambandham et al. (2014) found that an increase in chitosan dosage results in increased pollutant removal efficiencies since higher concentrations lead to higher reaction sites.

Figure 12 represents the effect of various chitosan concentrations and three different pH values on the % COD removal over 9 h period. A maximum COD removal of 55% was achieved at a pH of 2 and a chitosan dosage of 4.5 g/L. The % COD removal decreased as the pH increased from 2 to 6 and the % COD removal increased as the chitosan concentration increased from 2.5 g/L to 4.5 g/L.

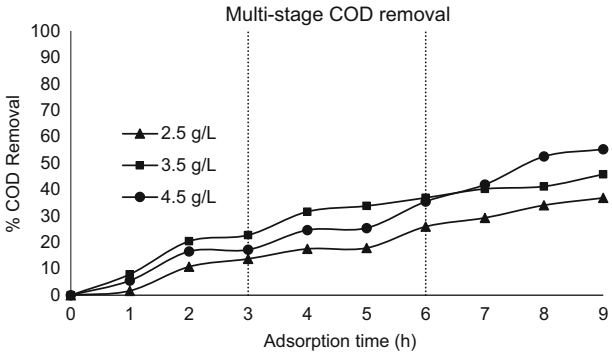


**Fig. 11** COD removal at adsorption stages

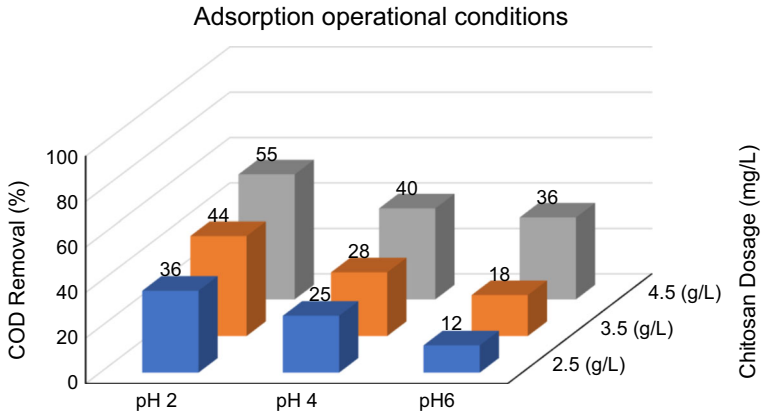


**Fig. 12** Adsorption operational parameters

The increased removal capacities at lower pH values are explained by the destabilization of oil molecules at strongly acidic conditions. Due to the structure of chitosan, the amine groups ($-NH^2$) are protonated which leads to interaction with anionic molecules in the water (Sokker et al. 2011). Similarly, an increase in protonated amine groups in the chitosan polymer induces a physical-chemical effect (Ruhsing Pan et al. 1999) which increases the droplet size of oil. This improves the adsorption of oil onto chitosan (Sakkayawong et al. 2005). The increase in adsorption capacity with an increase in chitosan concentration is due to more reaction sites available for pollutant removal (Thirugnanasambandham et al. 2014). However, according to Ahmad et al. (2005), this is only true for low concentrations since chitosan possesses a high charge density, and therefore, only low amounts are needed, since residual oil bind and bridge to chitosan molecules which destabilize the negatively charged colloids of residual oil through the charge neutralization mechanism.

### 3.4 Adsorption Isotherm

The data that was collected during the experiments, having initial COD concentrations ranging between 65,000 mg/L and 40,000 mg/L, were fitted using Langmuir, Freundlich, and Dubinin-Raduschkevich isotherms. The equilibrium adsorption isotherms are used to describe the interaction between solutes and adsorbents and assists in the design of adsorption systems (Chiou and Li 2002). The Langmuir and Freundlich models were applied initially; however, since these isotherms cannot reveal details pertaining to adsorption mechanism (Laus et al. 2010), the Dubinin-Raduschkevich isotherm (D-R) was also applied. The D-R isotherm is more general but analogous to the Langmuir isotherm. It does not assume a homogeneous surface or constant sorption potential (Aksoyoglu 1989). The D-R isotherm is used to identify whether chemical or physical adsorption mechanisms are followed by means of calculating the mean free energy of adsorption.

The following Langmuir isotherm, Eq. (2), was used to fit the experimental data (Laus et al. 2010):

$$q_e = \frac{q_m K_L C_e}{1 + K_L C_e} \tag{2}$$

where $C_e$ is the equilibrium solution concentration (mg/g), $q_e$ is the amount of COD adsorbed at the equilibrium (mg/g), $K_L$ is the Langmuir constant linked to the affinity of binding sites (L/mg) and $q_m$ is the practical limiting adsorption capacity (mg/g) when the surface of the adsorbent is completely covered with contaminant molecules. This allows for evaluation of adsorption performance (Chiou and Li 2002), $K_L$ and $q_m$ are calculated from a linearized form of Eq. (2) as shown in Eq. (3).

$$\frac{C_e}{q_e} = \frac{1}{q_m} C_e + \frac{1}{K_L q_m} \tag{3}$$

A linearized plot of ($C_e/q_e$) versus $C_e$ results in a straight line having a slope $1/q_m$ with intercept $1/q_mKL$ (Fig. 5). Calculated values are given in Table 5.

The important features of the Langmuir isotherm are represented by a dimensionless constant separation factor, $R_L$, shown in Table 5. $R_L$ is expressed by Eq. (4), where $C_0$ is the initial concentration of COD (mg/L) (Sokker et al. 2011).

$$R_L = \frac{1}{1 + K_L C_0} \tag{4}$$

The value of $R_L$ specifies whether the type of adsorption is unfavourable ($R_L > 1$), linear ($R_L = 1$), favourable ($0 < R_L < 1$) or irreversible ($R_L = 0$) (Bhatt et al. 2012; Bouberka et al. 2007). It was found that the $R_L$ values were favourable for all the isotherms since they were all between 0 and 1 (Table 5). As the chitosan concentration dosage increased from 2.5, 3.5 and 4.5 g/L, the corresponding $R_L$ values decreased to 0.698, 0.514 and 0.101, respectively, indicating favourable adsorption. Similar results were noted by Pitakpoolsil and Hunsom (2013). These results show that the affinity of the adsorbent for COD escalates when chitosan dosage increases.

The Freundlich isotherm is mathematically expressed as shown in Eq. (5) (Vázquez et al. 2007):

**Table 5** Langmuir, Freundlich and D-R isotherm constants for the adsorption of COD from biodiesel wastewater

| Parameters | | | |
|---|---|---|---|
| **Langmuir** | **2.5 g/L** | **3.5 g/L** | **4.5 g/L** |
| $R^2$ | 0.9895 | 0.9375 | 0.9995 |
| $q_m$ (mg/g) | 909.1 | 144.9 | 129.9 |
| $K_L$ (L/mg) | 0.000096 | 0.000163 | 0.00228 |
| $R_L$ | 0.698 | 0.514 | 0.101 |
| **Freundlich** | **2.5 g/L** | **3.5 g/L** | **4.5 g/L** |
| $R^2$ | 0.9982 | 0.9943 | 0.9998 |
| $n_f$ | 0.7562 | 2.647 | 0.2262 |
| $K_f$ | 1.379 | 1191.7 | 19.43 |
| **D-R** | **2.5 g/L** | **3.5 g/L** | **4.5 g/L** |
| $R^2$ | 0.9878 | 0.9994 | 0.9723 |
| $q_m$ (mg/g) | 1.94 | 20.07 | 1.10 |
| K ($mol^2/kJ^2$) | 14.224 | 22.402 | 11.584 |
| E (kJ/mol) | 0.187 | 0.149 | 0.208 |

$$Q_e = K_f C_e^{1/n} \tag{5}$$

This isotherm is typically used in cases of heterogeneous surface energy. This isotherm is characterized by the factor 1/n, related to heterogeneity. Whereas $q_e$ is the solid phase sorbate concentration at equilibrium (mg/g), $C_e$ is the liquid phase sorbate concentration (Salih and Gosh 2018) at equilibrium (mg/g), and $K_f$ is the Freundlich constant (Sokker et al. 2011). A linear form of the Freundlich isotherm can be obtained by taking logarithms of Eq. (5), as shown in Eq. (6):

$$\log q_e = \log K_F + \frac{1}{n}\log C_e \tag{6}$$

Therefore, a plot of linearized log $q_e$ versus log $C_e$ (Fig. 12) enables the constant $K_f$ and exponent 1/n to be determined, the calculated values are given in Table 5.

A value of $n = 1$ indicates linear adsorption, denoting that the adsorption sites are homogeneous (as in the Langmuir model) in energy and no interaction takes place between the adsorbed species. Values of $1/n < 1$ indicate favourable adsorption with an increase in sorption capacity, and that new adsorption sites occur. However, when 1/n is larger than 1 it shows that the adsorption bond is becoming weak and unfavourable adsorption takes place (Amiri et al. 2019). This results in decreased adsorption capacity (Özcan et al. 2004). Values of 1/n were found to be 0.756, 2.65 and 0.226 for dosages of 2.5, 3.5 and 4.5 g/L respectively. Therefore, adsorption was favourable at dosages of 2.5 and 4.5 g/L and unfavourable at 3.5 g/L. The Freundlich isotherm adequately describes the adsorption kinetics of COD onto chitosan. These results are consistent with those observed by Ahmad et al. (2005).

The Dubinin-Raduschkevich isotherm, Eq. (7), is used to calculate the mean free energy of sorption and predicts the nature of the adsorbate sorption onto the adsorbent (Kilislioglu and Bilgin 2003).

$$q_e = q_m \exp\left(-k\varepsilon^2\right) \tag{7}$$

where $C_e$ is the equilibrium solution concentration (mg/g), $q_e$ is the amount of COD adsorbed at the equilibrium (mg/g), K is a constant related to the adsorption energy ($mol^2/kJ^2$), $q_m$ is the theoretical saturation capacity (mg/g), ε is the Polanyi potential (J/mol) calculated with Eq. (8).

$$\varepsilon = RT \ln\left(1 + \frac{1}{C_e}\right) \tag{8}$$

The linear form of Eq. (10) is shown in Eq. (9):

$$\ln q_e = \ln q_m = k\varepsilon^2 \tag{9}$$

The values of $q_m$ and K are determined by plotting Ln($q_e$) versus $\varepsilon^2$ (Fig. 13), the values are presented in Table 5. The mean energy of adsorption (E) can be calculated from Eq. (10).

$$\mathrm{E} = (-2\mathrm{K})^{-1/2} \tag{10}$$

This parameter gives information about the adsorption mechanism as either chemical ion-exchange (8 kJ/mol < E < 16 kJ/mol) or physical adsorption (E < 8 kJ/mol) (Ozcan et al. 2005). Calculated values are shown in Table 5. Values of 0.187, 0.149 and 0.208 kJ/mol were

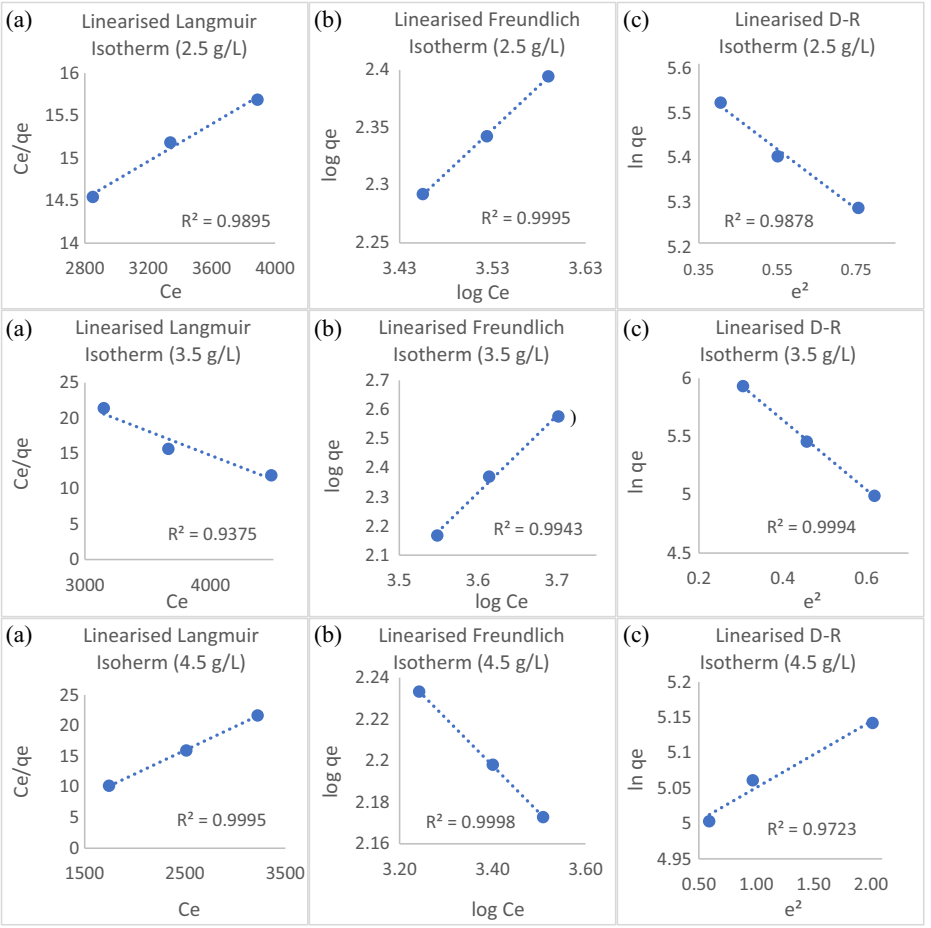


**Fig. 13** Linearized forms of the Langmuir, Freundlich and D-R models for the adsorption of COD at chitosan dosages of (a) 2.5 g/L; (b) 3.5 g/L; and (c) 4.5 g/L, with an initial wastewater pH of 2

observed at dosages of 2.5, 3.5 and 4.5 g/L, respectively, indicating that physical adsorption occurred at all chitosan dosages.

### 3.5 Integrated Treatment

The integrated treatment of biodiesel wastewater consisted of three consecutive treatment steps: (1) acidification; (2) electrochemical oxidation using $IrO_2$–$Ta_2O_5$ anodes; and (3) adsorption using chitosan as an adsorbent. The electrochemical oxidation of biodiesel wastewater was investigated at the start in order to determine the operating conditions that would result in the maximum COD removal. The same methodology was applied to the adsorption process. After the operating parameters of these two individual processes were established and pollutant removals were confirmed, then they were combined as consecutive steps in order to remove % of COD, FOG and BOD from industrial biodiesel wastewater in an integrated process. During the acidification step at a constant pH of 2, a % COD removal of 11% was achieved. The second step with the electrochemical oxidation process taking place over a 100-

h period at a current density of 1 mA/cm$^2$ and a NaCl concentration of 0.08 M reduced the % COD to almost 86%. During the third treatment step, adsorption with chitosan powder, at a pH of 2 and a chitosan dosage of 4.5 g/L, achieved 55% COD removal after three repetitive adsorption stages. These individual processes and their respective COD removal efficiencies are shown in Table 6.

The biodiesel wastewater effluent obtained after electrochemical oxidation in Experimental Run 3 was used as a feed for the third treatment step, adsorption using chitosan, at a pH of 2 and a chitosan dosage of 4.5 g/L for three consecutive steps. The result of this integrated treatment process is shown in Fig. 14.

The initial COD concentration of the raw biodiesel wastewater was 65,000 mg/L. After the first acidification step, the COD was reduced to 55,000 mg/L (11% COD removal). In the second step, during a 100-h period with an electrochemical oxidation cell at a current density of 1 mA/cm$^2$ and a NaCl concentration of 0.08 M the COD was further reduced to 7800 mg/L (86% COD removal). The final step of adsorption with chitosan where three consecutive adsorption stages at a pH of 2 and chitosan dosage of 4.5 g/L was followed, reduced the COD further to 3850 mg/L (51% COD removal). The decrease of the initial COD concentration of 65,000 mg/L to a final COD concentration of 3850 mg/L resulted in an overall % COD removal of 94%. Table 7 shows the final % BOD and FOG removal using this integrated process to 86% and 95% respectively.

A study completed by Siles et al. (2010) treated biodiesel wastewater with an integrated treatment process that consisted of acidification-electrocoagulation and anaerobic co-digestion. During this treatment process, the COD was reduced by 80% - 90%. Rattanapan et al. (2011) studied the treatment of biodiesel wastewater using an integrated treatment process consisting of acidification, coagulation and dissolved air flotation. This process was able to reduce FOG by 85% - 95% and COD by 40% - 50%. A combined electro-flotation and electro-oxidation process used in a study by Palomino Romero et al. (2013) showed that the system could successfully treat biodiesel wastewater using Ti/$RuO_2$ anodes. The COD was reduced by 95%, whereas FOG was completely removed.

This study confirms that an integrated process using acidification, electrochemical oxidation and adsorption using chitosan can reduce the COD, BOD and FOG according to the "City of Cape Town: Wastewater and Industrial Effluent By-law, 2013, discharge standards".

Figure 14 shows the COD concentration after each integrated step. A clear distinction can be seen between the untreated and treated wastewater when looking at the colour and clarity. There was no significant change in colour and clarity visible to the naked eye between the electrochemical and adsorption effluents.

Figure 15 shows the integrated system where COD concentration and % removal over the time intervals for each of the treatment processes. COD was reduced from 65,000 mg/L to 3850 mg/L after acidification, 100 h of electrochemical oxidation and three consecutive

**Table 6** Integrated treatment COD removal

| Process | COD (mg/L) | COD removal (%) |
|---|---|---|
| Initial | 65,000 | – |
| Acidification | 55,000 | 11 |
| Electrochemical oxidation | 7800 | 86 |
| Adsorption | 3850 | 55 |

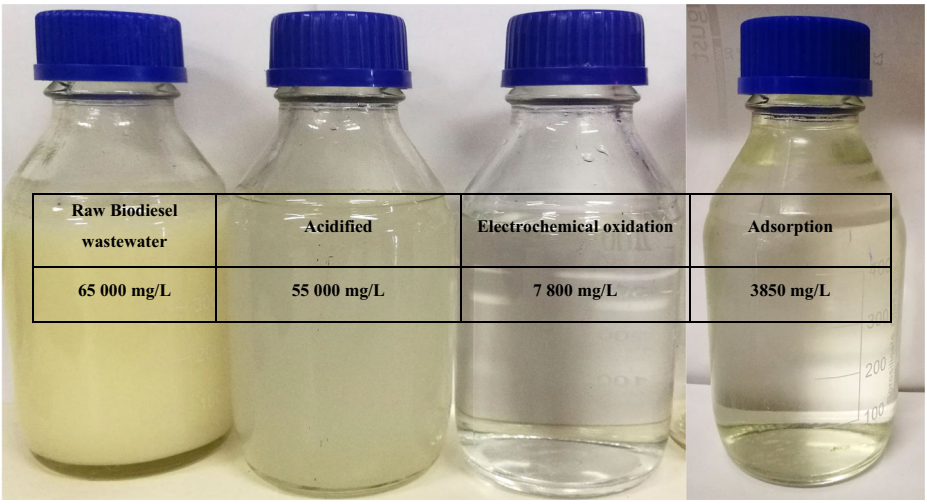


**Fig. 14** Wastewater after each respective treatment stage

adsorption stages, indicating successful treatment of industrial biodiesel wastewater using the integrated treatment process.

## 4 Conclusions

The integrated treatment process utilized in this study consisted of three consecutive steps: acidification, electrochemical oxidation, and adsorption. The treatment processes were investigated on a separate basis after which favourable conditions were combined into an integrated treatment process.

The first step, acidification, at a final pH of 2, removed the COD, BOD, and FOG by 11%, 10%, and 80%, respectively.

The second step, electrochemical oxidation, using a current density of 1 mA/cm$^2$, with a NaCl concentration of 0.08 M, showed excellent removal efficiencies. These conditions could reduce COD, BOD, and FOG by 86%, 88%, and 85%, respectively. The current density and NaCl concentrations had significant effects on the performance of the electrochemical oxidation process. This process was modelled using a central composite design. The proposed model could describe the process with a 90% accuracy level. The third and final step, adsorption using chitosan, showed favourable results when a chitosan concentration of 4.5 g/L at a pH of 2 was used. Three consecutive adsorption stages using fresh chitosan at these conditions resulted in a maximum of 55% COD, 54% BOD and 55% FOG removal. The

**Table 7** Integrated treatment process: Final pollutant concentrations

| Parameter | Initial (mg/L) | Final (mg/L) | Removal (%) | CCT:2013 |
|---|---|---|---|---|
| COD | 65,000 | 3850 | 94 | 5000 |
| BOD | 19,405 | 2620 | 86 | – |
| FOG | 265 | 12 | 95 | 4000 |

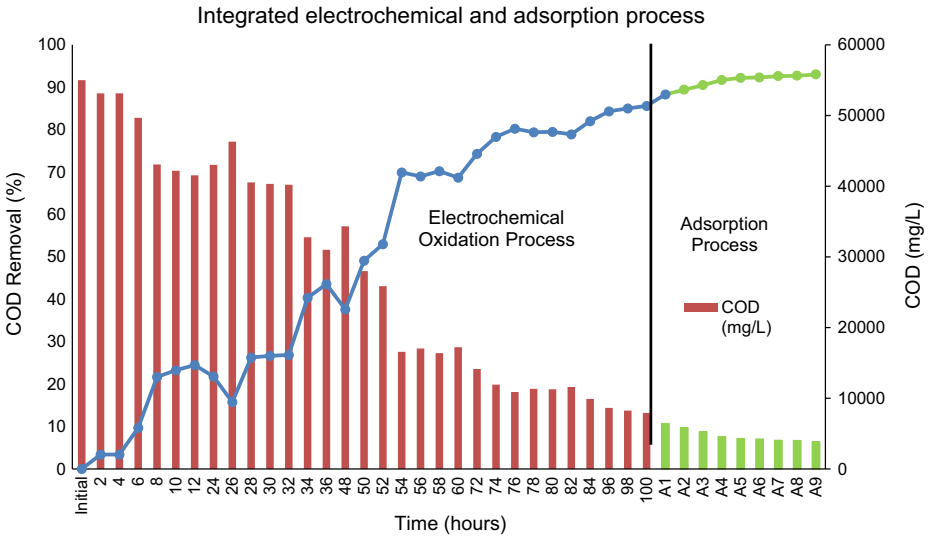


**Fig. 15** Integrated treatment COD removal over time

pH had a major impact on the performance of the process. Under acidic conditions, the COD % removal increased with an increase in chitosan concentration.

The integrated treatment process was able to reduce COD, BOD and FOG levels by 94%, 86% and 95%, respectively. This resulted in a treated effluent that complies with local industrial effluent discharge standards. Using this integrated process, the treated biodiesel wastewater effluent could be disposed of safely without further treatment.

**Acknowledgements** The National Research Foundation (NRF) of South Africa for the student scholarship. NMT Electrodes (PTY) Ltd., Durban, South Africa, for supplying the $IrO_2$–$Ta_2O_5$ anodes used in the electrochemical cell. The biodiesel producing company in Cape Town, South Africa, that supplied the industrial biodiesel wastewater effluent, used in this project.

## References

Ahmad AL, Sumathi S, Hameed BH (2005) Adsorption of residue oil from palm oil mill effluent using powder and flake chitosan: equilibrium and kinetic studies. Water Res 39:2483–2494. https://doi.org/10.1016/j.watres.2005.03.035

Aksoyoglu S (1989) Sorption of U(VI) on granite. J Radioanal Nucl Chem Artic 134:393–403. https://doi.org/10.1007/BF02278276

Almomani F, Baranova EA (2012) Electro-oxidation of two reactive azo dyes on a boron-doped diamond electrode. Water Sci Technol 66:465–471. https://doi.org/10.2166/wst.2012.180

Bhatt AS, Sakaria PL, Vasudevan M, Pawar PR, Sudheesh N, Bajaj HC, Mody HM (2012) Adsorption of an anionic dye from aqueous medium by organoclays: equilibrium modelling, kinetic and thermodynamic exploration. RSC Adv 2:8663. https://doi.org/10.1039/c2ra20347b

Bouberka AKZ, Kameche FSM, Derriche Z (2007) Adsorption study of an industrial dye by an organic clay. 149–158. https://doi.org/10.1007/s10450-007-9016-6

Chavalparit O, Ongwandee M (2009) Optimizing electrocoagulation process for the treatment of biodiesel wastewater using response surface methodology. J Environ Sci 21:1491–1496. https://doi.org/10.1016/S1001-0742(08)62445-6

Chiou MS, Li HY (2002) Equilibrium and kinetic modelling of adsorption of reactive dye on cross-linked chitosan beads. J Hazard Mater 93:233–248. https://doi.org/10.1016/S0304-3894(02)00030-4

Coledam DAC, Aquino JM, Rocha-Filho RC, Bocchi N, Biaggio SR (2014) Influence of chloride-mediated oxidation on the electrochemical degradation of the direct black 22 dye using boron-doped diamond and β-$PbO_2$ anodes. Quim Nova 37:1312–1317. https://doi.org/10.5935/0100-4042.20140219

Comninellis C (1994) Electrocatalysis in the electrochemical conversion/combustion of organic pollutants. Electrochim Acta 39:1857–1862

Costa NM, Silva VM, Damaceno G, Sousa RMF, Richter EM, Machado AEH, Trovó AG (2017) Integrating coagulation-flocculation and UV-C or H2O2/UV-C as alternatives for pre- or complete treatment of biodiesel effluents. J Environ Manag 203:229–236. https://doi.org/10.1016/j.jenvman.2017.07.069

Daud NM, Rozaimah S, Abdullah S, Hasan HA, Yaakob Z (2014) Production of biodiesel and its wastewater treatment technologies : a review. Process Saf Environ Prot 94:487–508. https://doi.org/10.1016/j.psep.2014.10.009

Daud Z, Awang H, Abdul Latif AA, Nasir N, Ridzuana MH, Ahmad Z (2015) Suspended solid, colour, COD and oil and grease removal from biodiesel wastewater by coagulation and flocculation processes. Procedia - Soc Behav Sci 195:2407–2411. https://doi.org/10.1016/j.sbspro.2015.06.234

De Marques Neto JO, Bellato CR, Milagres JL, Pessoa KD, de Alvarenga ES (2013) Preparation and evaluation of chitosan beads immobilized with iron(III) for the removal of as(III) and as(V) from water. J Braz Chem Soc 24:121–132. https://doi.org/10.1590/S0103-50532013000100017

Dewil R, Mantzavinos D, Poulios I, Rodrigo MA (2017) New perspectives for advanced oxidation processes. J Environ Manag 195:93–99. https://doi.org/10.1016/j.jenvman.2017.04.010

Fajardo AS, Seca HF, Martins RC (2017) Electrochemical oxidation of phenolic wastewaters using a batch-stirred reactor with NaCl electrolyte and Ti/$RuO_2$ anodes. J Electroanal Chem 785:180–189. https://doi.org/10.1016/j.jelechem.2016.12.033

Fazal MA, Haseeb ASMA, Masjuki HH (2011) Biodiesel feasibility study: an evaluation of material compatibility; performance; emission and engine durability. Renew Sust Energ Rev 15:1314–1324. https://doi.org/10.1016/j.rser.2010.10.004

Foley T, Thornton K, Dixon RK (2015) REN21. 2015. Renewables 2015 Global Status Report

Garcia-Segura S, Brillas E (2011) Mineralization of the recalcitrant oxalic and oxamic acids by electrochemical advanced oxidation processes using a boron-doped diamond anode. Water Res 45:2975–2984. https://doi.org/10.1016/j.watres.2011.03.017

Garcia-Segura S, Ocon JD, Chong MN (2018) Electrochemical oxidation remediation of real wastewater effluents — a review. Process Saf Environ Prot 113:48–67. https://doi.org/10.1016/j.psep.2017.09.014

Haseeb ASMA, Fazal MA, Jahirul MI, Masjuki HH (2011) Compatibility of automotive materials in biodiesel: a review. Fuel 90:922–931. https://doi.org/10.1016/j.fuel.2010.10.042

Huang CA, Yang SW, Chen CZ, Hsu F-Y (2017) Electrochemical behaviour of $IrO_2$ -$Ta_2$ $O_5$ /Ti anodes prepared with different surface pretreatments of Ti substrate. Surf Coatings Technol 320:270–278. https://doi.org/10.1016/j.surfcoat.2017.01.005

Jaruwat P, Kongjao S, Hunsom M (2010) Management of biodiesel wastewater by the combined processes of chemical recovery and electrochemical treatment. Energy Convers Manag 51:531–537. https://doi.org/10.1016/j.enconman.2009.10.018

Kilislioglu A, Bilgin B (2003) Thermodynamic and kinetic investigations of uranium adsorption on amberlite IR-118H resin. Appl Radiat Isot 58:155–160. https://doi.org/10.1016/S0969-8043(02)00316-0

Laus R, Costa TG, Szpoganicz B, Fávere VT (2010) Adsorption and desorption of cu(II), cd(II) and Pb(II) ions using chitosan crosslinked with epichlorohydrin-triphosphate as the adsorbent. J Hazard Mater 183:233–241. https://doi.org/10.1016/j.jhazmat.2010.07.016

Ltaïef AH, D'Angelo A, Ammar S, Gadri A, Galia A, Scialdone O (2017) Electrochemical treatment of aqueous solutions of catechol by various electrochemical advanced oxidation processes: effect of the process and of operating parameters. J Electroanal Chem 796:1–8. https://doi.org/10.1016/j.jelechem.2017.04.033

Moreira FC, Boaventura RAR, Brillas E, Vilar VJP (2017) Electrochemical advanced oxidation processes: a review on their application to synthetic and real wastewaters. Appl Catal B Environ 202:217–261. https://doi.org/10.1016/j.apcatb.2016.08.037

Ngamlerdpokin K, Kumjadpai S, Chatanon P (2011) Remediation of biodiesel wastewater by chemical- and electro-coagulation: a comparative study. J Environ Manag 92:2454–2460. https://doi.org/10.1016/j.jenvman.2011.05.006

Özcan AS, Erdem B, Özcan A (2004) Adsorption of Acid Blue 193 from aqueous solutions onto Na – bentonite and DTMA – bentonite. 280:44–54. doi: https://doi.org/10.1016/j.jcis.2004.07.035

Ozcan A, Ozcan A, Tunali S (2005) Determination of the equilibrium, kinetic and thermodynamic parameters of adsorption of copper(II) ions onto seeds of. J Hazard Mater 124:200–208. https://doi.org/10.1016/j.jhazmat.2005.05.007

Palomino Romero JA, Cardoso Junior FSS, Figueiredo RT, Silva DP, Cavalcanti EB (2013) Treatment of biodiesel wastewater by combined electroflotation and electrooxidation processes. Sep Sci Technol 48: 2073–2079. https://doi.org/10.1080/01496395.2013.779712

Pitakpoolsil W, Hunsom M (2013) Adsorption of pollutants from biodiesel wastewater using chitosan flakes. J Taiwan Inst Chem Eng 44:963–971. https://doi.org/10.1016/j.jtice.2013.02.009

Rajkumar D, Palanivelu K (2004) Electrochemical treatment of industrial wastewater. J Hazard Mater 113:123–129. https://doi.org/10.1016/j.jhazmat.2004.05.039

Rajkumar D, Kim JG, Palanivelu K (2005) Indirect electrochemical oxidation of phenol in the presence of chloride for wastewater treatment. Chem Eng Technol 28:98–105. https://doi.org/10.1002/ceat.200407002

Rattanapan C, Sawain A, Suksaroj T, Suksaroj C (2011) Enhanced efficiency of dissolved air flotation for biodiesel wastewater treatment by acidification and coagulation processes. Desalination 280:370–377. https://doi.org/10.1016/j.desal.2011.07.018

Ruhsing Pan J, Huang C, Chen S, Chung YC (1999) Evaluation of a modified chitosan biopolymer for coagulation of colloidal particles. Colloids Surface A Physicochem Eng Asp 147:359–364. https://doi.org/10.1016/S0927-7757(98)00588-3

Sakkayawong N, Thiravetyan P, Nakbanpote W (2005) Adsorption mechanism of synthetic reactive dye wastewater by chitosan. J Colloid Interface Sci 286:36–42. https://doi.org/10.1016/j.jcis.2005.01.020

Santos MRG, Goulart MOF, Tonholo J, Zanta CLPS (2006) The application of electrochemical technology to the remediation of oily wastewater. Chemosphere 64:393–399. https://doi.org/10.1016/j.chemosphere.2005.12.036

Sharma NK, Philip L (2016) Combined biological and photocatalytic treatment of real coke oven wastewater. Chem Eng J 295:20–28. https://doi.org/10.1016/j.cej.2016.03.031

Siles JA, Martin MA, Chica AF, Martin A (2010) Anaerobic co-digestion of glycerol and wastewater derived from biodiesel manufacturing. Bioresour Technol 101:6315–6321. https://doi.org/10.1016/j.biortech.2010.03.042

Sokker HH, El-Sawy NM, Hassan MA, El-Anadouli BE (2011) Adsorption of crude oil from aqueous solution by hydrogel of chitosan-based polyacrylamide prepared by radiation-induced graft polymerization. J Hazard Mater 190:359–365. https://doi.org/10.1016/j.jhazmat.2011.03.055

Suehara K, Kawamoto Y, Fujii E (2005) Biological treatment of wastewater discharged from biodiesel fuel production plant with alkali-catalyzed transesterification. J Biosci Bioeng 100:437–442. https://doi.org/10.1263/jbb.100.437

Sukkasem C, Laehlah S, Hniman A (2011) Upflow bio-filter circuit (UBFC): biocatalyst microbial fuel cell (MFC) configuration and application to biodiesel wastewater treatment. Bioresour Technol 102:10363–10370. https://doi.org/10.1016/j.biortech.2011.09.007

Thirugnanasambandham K, Sivakumar V, Prakash Maran J, Kandasamy S (2014) Chitosan-based grey wastewater treatment-a statistical design approach. Carbohydr Polym 99:593–600. https://doi.org/10.1016/j.carbpol.2013.08.058

Vázquez I, Rodríguez-Iglesias J, Marañón E, Castrillon L, Alvarez M (2007) Removal of residual phenols from coke wastewater by adsorption. J Hazard Mater 147:395–400. https://doi.org/10.1016/j.jhazmat.2007.01.019

Veljković VB, Stamenković OS, Tasić MB (2014) The wastewater treatment in the biodiesel production with alkali-catalyzed transesterification. Renew Sust Energ Rev 32:40–60. https://doi.org/10.1016/j.rser.2014.01.007

Wu W, Huang Z-H, Lim T-T (2014) Recent development of mixed metal oxide anodes for electrochemical oxidation of organic pollutants in water. Appl Catal A Gen 480:58–78. https://doi.org/10.1016/j.apcata.2014.04.035

Xu X, Cheng Y, Zhang T (2016) Treatment of pharmaceutical wastewater using interior micro-electrolysis/Fenton oxidation-coagulation and biological degradation. Chemosphere 152:23–30. https://doi.org/10.1016/j.chemosphere.2016.02.100

Yan Z, Zhao Y, Zhang Z (2015) A study on the performance of $IrO_2$-$Ta_2O_5$ coated anodes with surface-treated Ti substrates. Electrochim Acta 157:345–350. https://doi.org/10.1016/j.electacta.2015.01.005